ANYONS IN THE KITAEV MODEL

MAJ MEJAK

Fakulteta za matematiko in fiziko
Univerza v Ljubljani

In this paper, the topology of world lines is connected to basic statistic rules of elementary particles, and the possibility of anyons with intriguing statistical properties in two-dimensional worlds is discussed. Quantum spin liquids, characterized by an absence of local order parameter and fractionalized spin degrees of freedom, are presented as a candidate, where quasiparticle excitations in the form of anyons could occur. The exactly solvable Kitaev spin model on a honeycomb lattice, which predicts an emergence of a spin liquid ground state, is analysed in detail. Firstly, the physical background of frustrated bond-directional interactions is explored and the spin degrees of freedom are rewritten using Majorana fermions. The fractionalization of spins into static gauge fluxes and mobile Majorana fermions, forming two types of excitations, can be exploited as a signature of a spin liquid behaviour in experimental realizations of the Kitaev model. Lastly, measurements of specific heat and dependence of the spin excitation gap on the external magnetic field in the Kitaev material α-$RuCl_3$ are shown as experimental results that support theoretical predictions of spin fractionalization.

ANYONI V MODELU KITAEVA

V članku je predstavljena zveza med topologijo svetovnic v prostor-času ter statističnimi pravili elementarnih delcev. V dvodimenzionalnih sistemih drugačne topološke lastnosti svetovnic omogočajo pojav anyonov s posebnimi statističnimi lastnostmi. Teoretični modeli kvantnih spinskih tekočin, za katere je značilna odsotnost lokalnega ureditvenega parametra, napovedujejo možnost pojava kvazi-delčnih vzbuditev z anyonsko statistiko. V članku je podrobneje predstavljen analitično rešljiv model Kitaeva na satovju, ki ima lastnosti kvantnih spinskih tekočin. Sprva je opisano fizikalno ozadje anizotropnih usmerjenih interakcij med spini, ki izvirajo iz specifične geometrije kristalne rešetke, z vpeljavo Majoranovih fermionov pa so nadomeščene originalne spinske prostostne stopnje. Frakcionalizacija spinskih prostostnih stopenj v dve različni vrsti vzbuditev je temeljni pokazatelj fizike kvantnih spinskih tekočin v eksperimentalnih realizacijah modela Kitaeva. Nazadnje so prikazane meritve specifične toplote ter odvisnosti eksitacijske reže od zunanjega magnetnega polja v materialu α-$RuCl_3$, ki se skladajo s teoretičnimi napovedi spinske frakcionalizacije.

1. Introduction

It is remarkable how properties of elementary particles can be traced back to indistinguishability and topology of motion in space-time [1]. Both these basic principles are responsible for all elementary particles in our three-dimensional world being either fermions or bosons. One would expect the same for systems in fewer dimensions, however, the topology in two dimensions is richer, allowing particles called anyons, which obey intriguing statistical properties intermediate between bosons and fermions.

Material science presents an insightful new playground, in which exotic new particles are being realized in the form of quasiparticle excitations. Particularly interesting are systems of entangled spins coupled with frustrating exchange interactions, where magnetic order is absent down to zero temperature. Such states are called quantum spin liquids and have gained a lot of attention from experimental physicists, who are striving to observe signs of quasiparticle excitations in real physical systems. Quantum spin liquids can exhibit fractionalization of the spin degrees of freedom into quasiparticle excitations with interesting statistics. The ground spin liquid state is profoundly different from conventional magnetically ordered ground states, since it has no magnetic order, even though the spins are strongly interacting. The absence of the local order parameter makes spin liquids even harder to observe in experiment. The Kitaev honeycomb model, discussed in this paper, is one of few exactly solved 2D models that predict a quantum spin liquid ground state. The system is predicted to host a Z_2 gauge field and Majorana fermions, both corresponding to different types of excitations. A Majorana fermion has an interesting property that it is its own antiparticle, whereas the excitations of the Z_2 gauge field obey anyonic statistics. Recent advances in preparation of two-dimensional samples have enabled researchers to find signatures of two types of quasiparticle excitations in the Kitaev material α-$RuCl_3$ [2]. The search for a solid-state realization of the Kitaev honeycomb model is driven by a potential application in quantum computing technologies and deeply inspired by the fundamental pursuit of spin liquid materials as well as the experimental discovery of Majorana fermions.

2. Anyons and topology of space-time

Quantum statistics of a system of indistinguishable particles refers to the topology of world lines in space-time, which is profoundly different for systems with fewer spatial dimensions. Every permutation of indistinguishable particles should represent the same state of a many body system and should not change any physical observable [3]. When introducing anyonic particles, we shall focus on the case of Abelian anyons, where an interchange of any two particles in the system $\psi_1 \leftrightarrow \psi_2$ causes the wave function to acquire only a global phase factor $e^{i\theta}$, which does not result in any measurable difference.

$$|\psi_1\rangle_1 |\psi_2\rangle_2 = e^{i\theta} |\psi_2\rangle_1 |\psi_1\rangle_2 \,. \tag{1}$$

In three spatial dimensions, there is only one topologically distinct way to swap two particles. Two consecutive swaps are equivalent to the identity transformation, allowing only two possible values of the phase factor $e^{i\theta} = \pm 1$. Thus, elementary particles in three dimensions are either fermions, whose phase factor is -1, or bosons, whose phase factor is $+1$. The phase factor -1 takes care that fermions obey the Pauli exclusion principle, which forbids two fermions from being in the same quantum state at the same time (Figure 1).

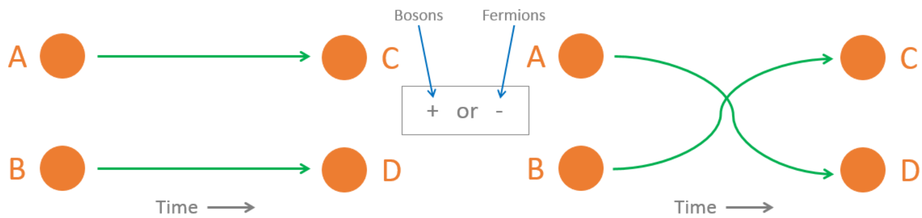

Figure 1. The wave function of the final state of two indistinguishable particles at points C and D must include contributions from every possible motion connecting the starting positions to the end points. The options fall into two topologically distinct classes; the way we combine the two contributions either by adding or subtracting gives us bosons (+) or fermions (−) (Reproduced from [1]).

Anyons, first hypothesised by Wilczek [1], are particularly intriguing particles, since they exhibit quantum statistics intermediate between bosons and fermions, where the phase θ upon exchange can take any value, hence the name anyon. Such intermediate statistics is possible only for indistinguishable particles in two dimensions. In a world of two spatial dimensions, the topology of pairs (or larger groups) of world lines becomes much richer than in worlds of three or more spatial dimensions. The reason is closely connected to a basic feature of knots, which cannot form in more than three dimensions [1]. In mathematics, a knot is just a closed continuous curve in space. Untangling a knot requires points on the curve, labelled with numbers on interval $[0, 1)$, to flow continuously to points on a circle with the corresponding number. Obstructions in unravelling might arise when different parts of the knot come to intersect, however, in four or more dimensions we can always move two strands past one another. In a two-dimensional system with three-dimensional space-time world lines of particles can produce an infinite number of topologically distinct trajectories that could in principle lead to any value of the phase θ (Figure 2).

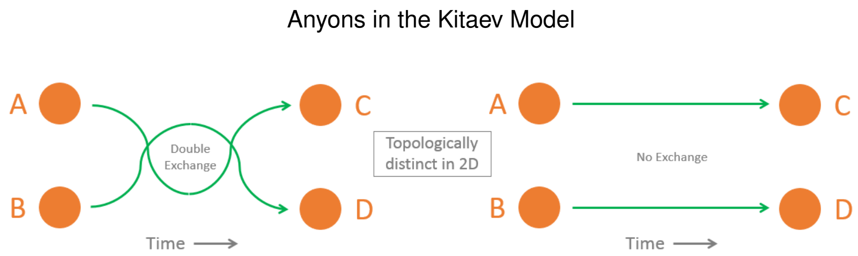

Figure 2. One particle exchange is followed by another resulting in double exchange (left) which is not topologically equivalent to identity (right) in three-dimensional space-time. The two paths can wind up around one another and cannot be unravelled by continuous motion (Reproduced from [1]).

Even more exotic properties emerge when interchanging non-Abelian anyons, where braiding (exchanging) two anyonic particles acts as a unitary transformation within a multidimensional degenerate Hilbert subspace. The resulting wave function cannot be connected to the initial one just by a global phase factor. Since anyonic statistics is possible only in two dimensions, the quest of finding anyons turned towards material science, where exotic new particles are being realized in the form of quasiparticle excitations of electrons in quantum materials [4]. A well known example of a quasiparticle excitation in ordered (anti)ferromagnetic spin systems are magnons that obey bosonic statistics. Consequently, magnons exhibit quite different properties than spins. Every spin flip is decomposed into linear combination of stable quasiparticles (magnons) that retain their identity even when they propagate [5]. Especially interesting are quasiparticle excitations in states of highly entangled electrons, where electrons are not confined in place by any bonds as in solids, but are still correlated due to quantum entanglement as opposed to electron gas. Excitations formed in these systems are quasiparticles that can even possess anyonic properties [1]. First example that suggested such a behaviour was found in fractional quantum Hall fluid [6], where electrons, confined to a two-dimensional layer, are taken to extremely low temperatures and subjected to large magnetic fields. The emergent quasiparticle excitations in those liquids typically behave like one-third of an electron; they carry one third of its charge and exhibit one third of fermion statistics. Their amplitude for interchange will be multiplied by a phase factor $e^{i\pi/3}$ [1]. Unfortunately, experimental measurements of anyonic quasiparticles in such systems suffer from many practical obstacles. It might in principle be easier to observe them in materials called quantum spin liquids, where the electrons remain static and their spin dynamics defines the physics [4].

3. Quantum spin liquids

Quantum spin liquids can be formed by interacting spins and offer a significantly different behaviour than typical magnetic materials. Spin liquids lie between ordinary magnets (spin solids), in which the directions of spins are rigidly aligned, and paramagnets (spin gases), in which the spin orientations are almost completely independent of one another. Spins in typical magnetic materials experience a disordered state at higher temperatures and begin to align into ordered patterns (domains, stripes etc.) at lower temperatures [5]. In contrast, a quantum spin liquid is characterized by an absence of magnetic long-range order (although interactions and correlations are strong) down to zero temperature as well as by their long-range quantum entanglement and fractionalized excitations of the spin degrees of freedom [7].

3.1 Frustration in magnetic systems

Spin liquid states are predicted to occur in frustrated magnetic systems. Frustration in magnetic systems arises in the case of competing exchange interactions, whose energies cannot be minimized at the same time. Frustration may occur as a consequence of the spin lattice geometry, the simplest example being an antiferromagnetic system on a two dimensional triangular lattice. We call this phenomenon geometric frustration and is common in spin systems on pyrochlore, kagome or triangular lattices [2]. On the other hand, the discussed Kitaev model on a honeycomb lattice (Figure 3) exhibits exchange frustration as a result of bond-directional interactions [8], where the exchange easy-axis of Ising-like interactions differs depending on the orientation of the bond between the spins. The geometry of the honeycomb lattice is bipartite, since it can be divided into two sublattices where sites on either of the sublattices interact only with sites in the other sublattice [5]. For example, if all the interactions between spins shared the same exchange easy-axis, there would be no magnetic frustration on a honeycomb lattice.

(a) **(b)**

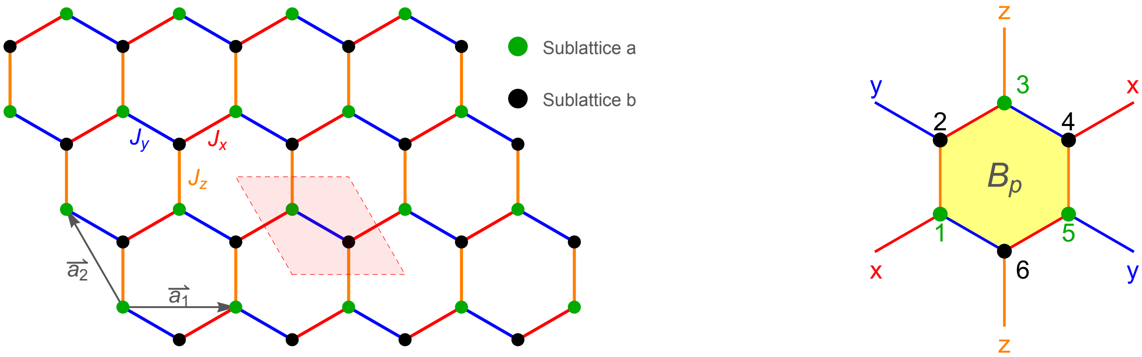

Figure 3. **(a)** A bipartite honeycomb lattice of spins is constructed by two equivalent sublattices a and b with primitive vectors $\vec{a}_1$ and $\vec{a}_2$. The unit cell is depicted by a red rhombus. The bonds between the nearest neighbouring spins are divided into three types each with a different exchange coupling J_α and exchange easy-axis. **(b)** An elementary hexagonal plaquette B_p with a particular enumeration of the sites used in definition (3).

3.2 Resonating valence bond state

First theoretical construction of a spin liquid originates from the resonating valence bond theory of frustrated antiferromagnets, proposed by Anderson in 1973 [9]. In order to construct a ground state with zero magnetic moment in a system with antiferromagnetic interactions, two electron spins can be joined to form a spin singlet $\frac{1}{\sqrt{2}}(|\uparrow\downarrow\rangle - |\downarrow\uparrow\rangle)$. If every spin in the system is bound in a singlet, the state of the system as a whole has zero spin and no magnetic order. Static configuration of spin singlets is called a valence bond solid (Figure 4.a). However, coupling of spins in a particular distribution of singlets breaks the lattice symmetry and possesses no long-range entanglement that is predicted in the spin liquid states [7]. To preserve the symmetry, a superposition of many different partitionings of spins into singlets is used to construct the ground state, known as the resonating valence bond state, which can support some exotic excitations; one example is the spinon excitation (Figure 4.b), which is created when a spin is not paired in a valence bond pair. The spinon possesses no electric charge and obeys fermionic statistics. A spinon can move by rearranging nearby valence bonds at low energy cost [10].

(a) **(b)**

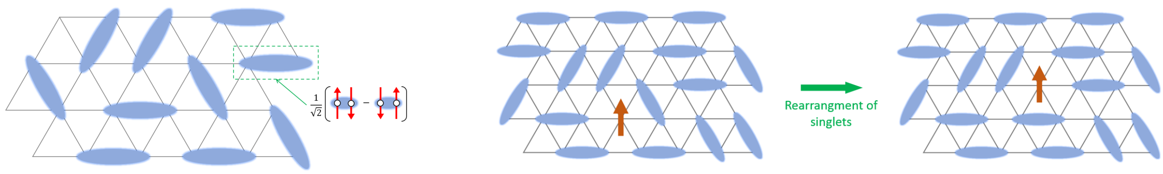

Figure 4. **(a)** Valence bond solid on a geometrically frustrated triangular lattice with antiferromagnetic exchange interaction. **(b)** Excitation of a spinon can propagate through a valence bond solid simply by rearrangements of singlet pairs.

4. Kitaev Model

The Kitaev spin model, consisting of a network of spins on a honeycomb lattice (Figure 3), represents an exactly solvable frustrated spin system with the exact quantum spin liquid ground state. As we shall see, the original spin degrees of freedom σ_i fractionalize into propagating quasiparticles, which turn out to behave as Majorana fermions, and a static Z_2 gauge field. The spin liquid state also possesses no magnetic order, however, the entanglement of spins spreads through the entire network of spins. A detailed derivation of the model was presented in a seminal work by Alexei Kitaev in 2006 [11]. He studied a system of N spins 1/2 located at vertices of a honeycomb lattice. The interaction between two neighbouring spins is Ising-like, $\sigma_i^\alpha \sigma_j^\alpha$, however, the exchange easy axis α and the magnitude of the interaction J_α depend on the spatial orientation of the exchange bond. The Hamiltonian is as follows:

$$H = -\,J_x \sum_{x-\text{links}} \sigma_i^x \sigma_j^x - J_y \sum_{y-\text{links}} \sigma_i^y \sigma_j^y - J_z \sum_{z-\text{links}} \sigma_i^z \sigma_j^z. \tag{2}$$

4.1 Physical background of the Kitaev interaction

Bond-directional Ising interactions that result in spin liquid behaviour in the Kitaev honeycomb model are caused by interacting $j = 1/2$ spins in Mott insulators. Mott insulators are materials with strong interactions between electrons, which create an energy gap failed to be correctly described by conventional band theories that predict a partially filled valence band [12]. Such states are usually formed in transition-metal oxides with partially filled d_4 or d_5 orbitals, where an interplay of crystal-field effects, strong spin-orbit coupling and electron interactions leads to coupled $j = 1/2$ spin transition-metal ions [8]. Microscopic origins of bond-directional exchange interactions were pioneered by Jackeli and Khaliullin [13], who studied exchange interactions between IrO_6 octahedra. The exchange interaction between neighbouring magnetic moments of Ir^{4+} ions depends on the geometric orientation of the neighbouring octahedra (Figure 5).

(a) **(b)** **(c)**

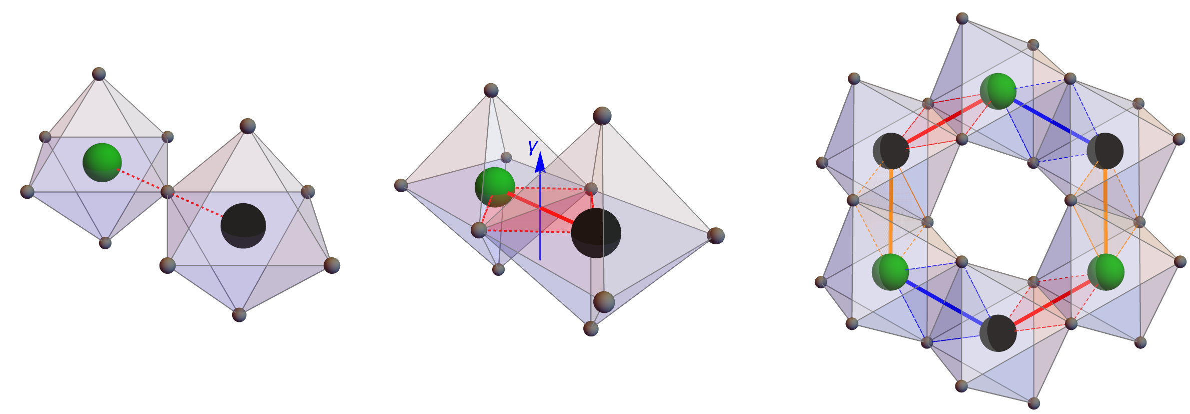

Isotropic Heisenberg interaction $J\ \vec{S}_i \cdot \vec{S}_j$

Bond-directional interaction $J_\gamma\ S_i^\gamma \cdot S_j^\gamma$

Configuration of six IrO_6 octahedra, forming a honeycomb lattice.

Figure 5. Possible geometric orientations of neighbouring IrO_6 octahedra that give rise to different types of (dominant) exchange interactions between the magnetic moments located on the iridium ion at the centre of the octahedra. **(a)** For the corner-sharing geometry one finds a dominant symmetric Heisenberg exchange. **(b)** For the edge-sharing geometry one finds a dominant bond-directional, Kitaev-type exchange. **(c)** Edge sharing octahedra can be configured so that their centres (transition metal ions) form a honeycomb lattice. The planes (red, orange and blue rhombi) spanned by different types of exchange paths α (red, orange and blue lines) are perpendicular to one another.

The edge sharing configuration has two exchange paths between neighbouring iridium ions resulting in a destructive interference of the isotropic Heisenberg exchange between coupled $j = 1/2$ states. The bond-directionality of the coupling arises, because the two linked d orbitals of the Iridium ions in neighbouring octahedra depend on the directionality of the edge, shared by the two octahedra. The corresponding exchange easy-axis α of the Ising interaction $\sigma_i^\alpha \sigma_j^\alpha$ is perpendicular to the plane spanned by the two exchange paths [8]. Apart from the pure Kitaev interaction, other non-trivial couplings in the system may cause realistic systems to still exhibit magnetic ordering at sufficiently low temperatures. However, the system becomes a conventional paramagnet only at significantly higher temperatures than the onset of the ordered phase, indicating an intermediate phase without any magnetic order but with short-range spin correlations [2].

4.2 Conserved quantities of the model

Before transforming the spin model into a system of interacting Majorana fermions, we observe the presence of a large number of conserved quantities. For each hexagon (Figure 3) we can define a plaquette operator B_p, which commutes with the Hamiltonian (2):

$$B_p = \sigma_1^x \sigma_2^y \sigma_3^z \sigma_4^x \sigma_5^y \sigma_6^z, \qquad [B_p, H] = 0, \qquad [B_p, B_q] = 0. \tag{3}$$

The fact $B_p^2 = 1$ also implies that eigenvalues of B_p are ± 1 [14].

4.3 Majorana fermions

Fermionic or bosonic field operators are commonly used to express the spin 1/2 algebra of a 2^N dimensional Hilbert space in a Hamiltonian [3]. Kitaev [11] used a fermionisation procedure where Pauli matrices are expressed via Majorana operators. Each fermionic mode k is usually described by a creation operator $a_k^\dagger$ and an annihilation operator a_k. Instead, one can use their linear combinations:

$$c_{k,1} = a_k + a_k^\dagger, \qquad c_{k,2} = \frac{1}{i}\left(a_k - a_k^\dagger\right), \tag{4}$$

which are called Majorana operators, since they obey the following relations:

$$c_i^\dagger = c_i, \qquad \{c_i, c_j\} = 2\delta_{i,j}, \tag{5}$$

making each Majorana particle a fermion that is its own antiparticle. Each spin on the site j is represented by four Majorana operators c_j, c_j^x, c_j^y, c_j^z (Figure 6), which are defined by linear combinations (4) using two fermionic modes $a_j^{(1)}$, $a_j^{(2)}$. By representing each spin with four Majorana operators, we have expanded the Hilbert space from a 2^N dimensional space to the extended space $\mathcal{M}$ with dimension $2^N \cdot 2^N = 4^N$. Actual physical spin states occupy only a subspace of the extended space of four Majorana fermions per site [11]. We use the following definition:

$$\widetilde{\sigma}_j^x = i c_j^x c_j, \qquad \widetilde{\sigma}_j^y = i c_j^y c_j, \qquad \widetilde{\sigma}_j^z = i c_j^z c_j, \tag{6}$$

to define the Pauli operators in the extended space [11]. A state $|\Psi\rangle$ belongs to the physical subspace $\mathcal{P} \subset \mathcal{M}$, only if the operator D_j (7), with eignevalues ± 1, acts on the state $|\Psi\rangle$ consistently with Pauli matrices $\sigma_j^x \sigma_j^y \sigma_j^z = i$ [11].

$$iD_j = i c_j^x c_j^y c_j^z c_j = \widetilde{\sigma}_j^x \widetilde{\sigma}_j^y \widetilde{\sigma}_j^z, \qquad (D_j)^2 = 1. \tag{7}$$

Consequently, a state $|\Psi\rangle$ in the physical subspace $\mathcal{P}$ must be an eigenstate of all D_j with eigenvalue $+1$: $D_j |\Psi\rangle = |\Psi\rangle$. For every state $|\Psi\rangle$ in the extended space $\mathcal{M}$ one can obtain the corresponding physical state $|\Psi\rangle_{\text{phy}} = P |\Psi\rangle$ by applying the projection operator $P = \prod_j \frac{1+D_j}{2}$. One can show that the Pauli operators defined with Majorana modes (6) preserve the commutation relation for Pauli matrices only on the physical subspace $|\Psi\rangle \in \mathcal{P}$ [11]:

$$\left[\widetilde{\sigma}_j^{\alpha}, \widetilde{\sigma}_j^{\beta}\right] \ |\Psi\rangle = 2i \ \varepsilon_{\alpha\beta\gamma} \ \widetilde{\sigma}_j^{\gamma} \ |\Psi\rangle \,. \tag{8}$$

We combine two Majorana operators on neighbouring sites to define the Z_2 gauge field operators u_{ij}^{α} [11]:

$$u_{ij}^{\alpha} = i c_{i,a}^{\alpha} c_{j,b}^{\alpha}, \qquad \left(u_{ij}^{\alpha}\right)^2 = 1, \tag{9}$$

where index a and b denote the sublattice and $\alpha \in \{x, y, z\}$ denotes the bond type. The Hamiltonian (2) is rewritten in quadratic form in Majorana operators c_k:

$$H = J_x \sum_{x-\text{links}} u_{ij}^{x} \ i \ c_{i,a} c_{j,b} + J_y \sum_{y-\text{links}} u_{ij}^{y} \ i \ c_{i,a} c_{j,b} + J_z \sum_{z-\text{links}} u_{ij}^{z} \ i \ c_{i,a} c_{j,b}. \tag{10}$$

The field operators u_{ij}^{α} represent conserved quantities with eigenvalues ± 1, since they commute with the Hamiltonian and with each other [11]:

$$\left[u_{ij}^{\alpha}, H\right] = 0, \qquad \left[u_{ij}^{\alpha}, u_{ij}^{\beta}\right] = 0. \tag{11}$$

(a) **(b)**

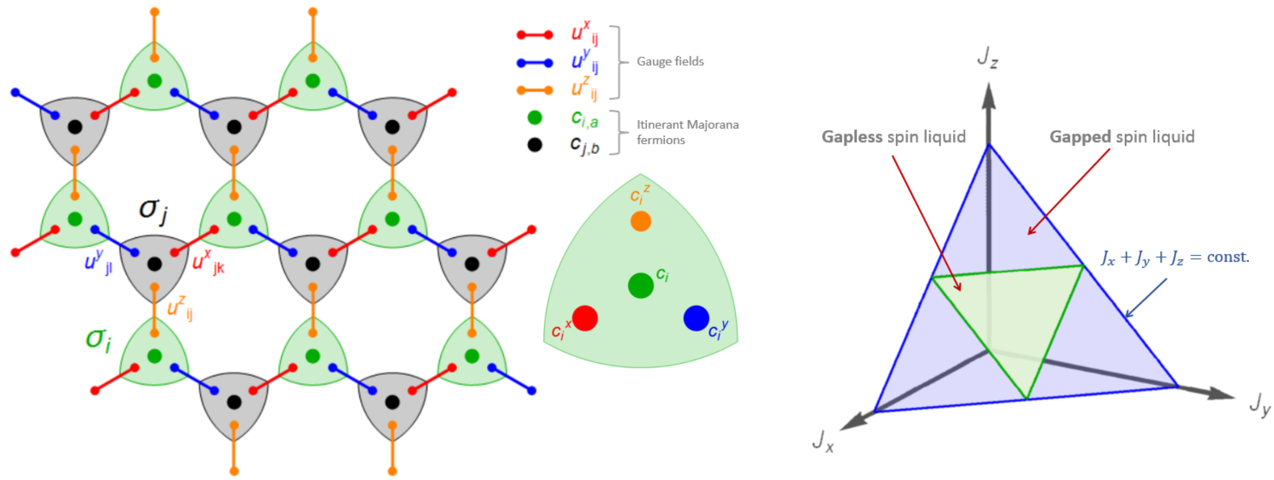

Figure 6. **(a)** Graphical representation of spin operators σ_i with four flavours of Majorana fermions, which are recombined into statical Z_2 gauge fields u_{ij}^{α} and itinerant Majorana fermions $c_{i,a(b)}$. **(b)** Phase diagram of the Kitaev model, plotted for a plane $J_x + J_y + J_z = \text{const.}$ If one of the couplings dominates, a gapped spin liquid is formed. Around isotropic coupling strengths, a gapless spin liquid state is formed (Majorana metal) [8].

In the original Hamiltonian (2), there are no conserved quantities associated directly with bonds, only the plaquette operators B_p represent physical observables and can be expressed by a product of six gauge field operators u_{ij}^{α}, one for each bond $(i,j)_\alpha$, along the boundary of the hexagon ∂B_p:

$$B_p = \prod_{(i,j)_\alpha \in \partial B_p} u_{ij}^{\alpha}. \tag{12}$$

Operators u_{ij}^{α} are called gauge fields, since there are many distinct choices of their eigenvalues that yield the same configurations of plaquettes $B_p = \pm 1$. The energy of the system does not directly depend on u_{ij}^{α}, rather it is related to distribution of plaquettes [11]. For every unique distribution of gauge fields u_{ij}^{α} we have to solve a slightly different, but profoundly simplified Hamiltonian (10), which has been the initial goal of introducing Majorana operators.

4.4 Ground state and energy spectrum

Every distinct distribution of plaquette eigenvalues yields different energies of the quadratic Majorana Hamiltonian (10). It turns out that uniform distribution of plaquettes $B_p = 1$ yields a global minimum of the energy spectrum [11]. Setting all $u_{ij}^{\alpha} = 1$ is one of many choices of gauge fields that yield the uniform distribution. The corresponding Hamiltonian is translational invariant and can be diagonalized by Fourier transformation $c_{i,a(b)} \to c_{\vec{k},a(b)}$ in momentum representation $\vec{k}$ [11]. The diagonalised Hamiltonian has the form:

$$H = \frac{1}{4} \sum_{\vec{k} \in \mathrm{BZ}} \varepsilon_{\vec{k}} \left(\alpha_{\vec{k}}^{\dagger} \alpha_{\vec{k}} - \beta_{\vec{k}}^{\dagger} \beta_{\vec{k}} \right), \qquad \varepsilon_{\vec{k}} = 2 \left| J_z + J_x e^{-i\vec{k}\cdot\vec{n_1}} + J_y e^{-i\vec{k}\cdot\vec{n_2}} \right|, \qquad \vec{n_{1,2}} = \pm\frac{1}{2}\vec{e}_x + \frac{\sqrt{3}}{2}\vec{e}_y, \tag{13}$$

where the sum goes over the first Brillouin zone $\vec{k} \in \mathrm{BZ}$ [11]. The energy $\varepsilon_{\vec{k}}$ is associated with new quasiparticle field operators $\alpha_{\vec{k}}$ and $\beta_{\vec{k}}$, introduced by unitary transformation of momentum Majorana operators $c_{\vec{k},a(b)}$ [11].

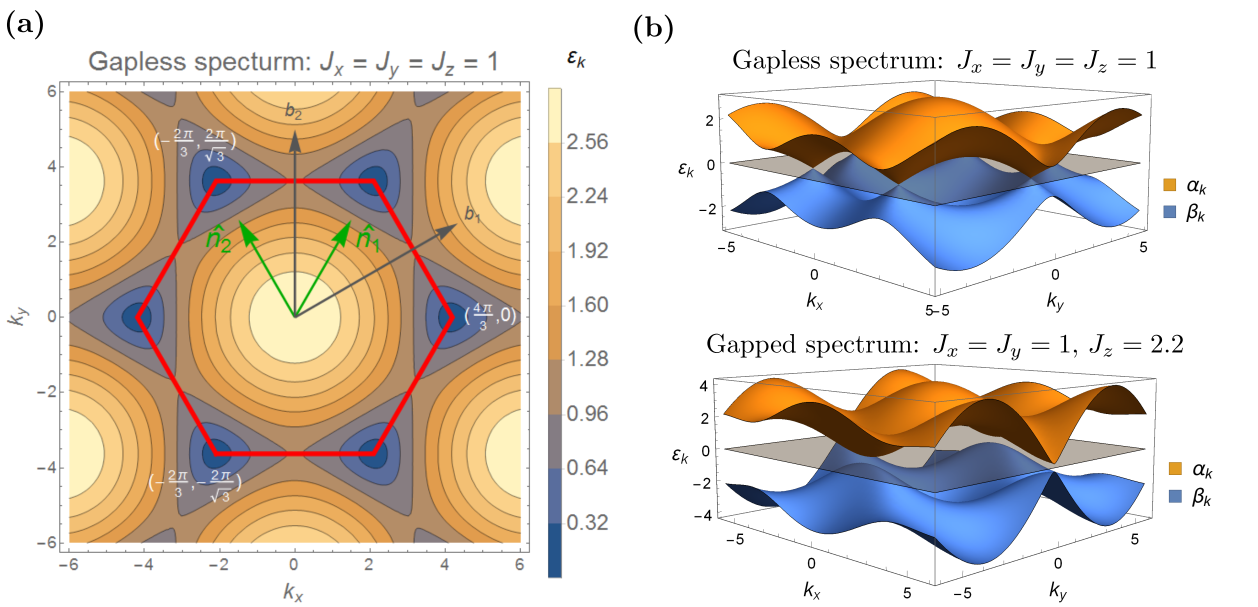

Figure 7. (a) Dispersion relation $\varepsilon_{\vec{k}}$ of the gapless spin liquid state, depicted in the first Brillouin zone (red hexagon). The energy gap vanishes at six vertices of the Brillouin zone, where the dispersion is linear. Green arrows denote unit vectors $\vec{n_{1,2}} = \pm\frac{1}{2}\vec{e}_x + \frac{\sqrt{3}}{2}\vec{e}_y$ used in dispersion relation (13). **(b)** Dispersion relation for the gapless phase (above) and for the gapped phase (below), where the dispersion is quadratic near minima.

The spin liquid ground state is obtained by filling all the negative energy states $\beta_{\vec{k}}$ with quasiparticles. The energy spectrum can be either gapped or not depending on the parameters J_α of the dispersion relation $\varepsilon_{\vec{k}}$ (Figure 7). The spectrum is gapless, if $\varepsilon_{\vec{k}} = 0$ for some $\vec{k} \in \mathrm{BZ}$. This is possible only if all the triangle inequalities for exchange couplings $|J_\alpha| \le |J_\beta| + |J_\gamma|$ hold (see Figure 6). The excitations of Kitaev spin liquid can be divided into Z_2 flux excitations, triggered by changing the uniform distribution of plaquettes $B_p = 1$ in the ground state, and excitations of the itinerant Majorana fermions. The magnitude of these two types of excitations differ and are excited at different temperatures, which was also observed experimentally in Kitaev materials [2]. In the gapless phase, the low energy excitations are itinerant Majorana fermions, whereas in the gapped phase the low energy excitations correspond to Z_2 flux excitations, which turn out to behave as Abelian anyons. In fact, one can explicitly map the gapped phase of the Honeycomb model to the famous Toric code model of spins on the square lattice [15], which is known to host three different types of deconfined anyonic excitations; charge e excitations, vortex m excitations and combined fermionic $\varepsilon = e \times m$ excitations. They are characterized by special braiding rules when they are interchanged; e and m anyons obey bosonic statistics in respect to themselves and the ε anyon obeys fermionic statistics. However, if we move one e excitation in a loop around an m excitation, the wavefunction acquires an additional -1 phase factor [15]. Both models lead to similar physics, however, the Honeycomb model has much more potential to be experimentally realized, since the quartic spin interactions in the Toric code model are very unlikely to appear in a real physical system. The gapless phase also acquires an energy gap when exposed to the external magnetic field; the emergent quasiparticle excitations are even more exotic non-Abelian anyons, which correspond to a multi-dimensional representation of the braid group [11].

4.5 Order parameter and spin correlations

We can combine two Majorana fermions forming a gauge field u_{ij}^{α} to define a bond fermion operator $\eta_{(ij),\alpha}$, used to express spin operators σ_i [14]:

$$\eta_{(ij),\alpha} = c_{i,a}^{\alpha} + i c_{j,b}^{\alpha}, \qquad \sigma_{i,a}^{\alpha} = i\left(\eta_{(ij),\alpha} + \eta_{(ij),\alpha}^{\dagger}\right) c_{i,a}, \qquad \sigma_{j,b}^{\alpha} = i\left(\eta_{(ij),\alpha} - \eta_{(ij),\alpha}^{\dagger}\right) c_{j,b}. \tag{14}$$

A spin operator σ_i^{α} (6) creates a Majorana fermion c_i and affects the α bond with the nearest neighbour σ_j^{α}, changing the occupation number of the bond fermion $\eta_{(ij),\alpha}$, which is expressed by creation of two Z_2 fluxes at adjacent plaquettes. We say that the original spin degree of freedom fracitonalizes into Majorana fermion and two static Z_2 fluxes [11] (Figure 8).

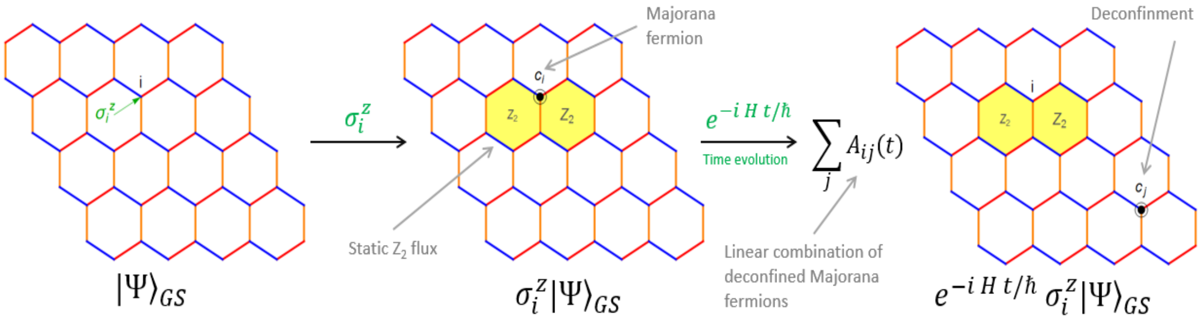

Figure 8. Fractionalization of a spin into two static Z_2 fluxes and a dynamic itinerant Majorana fermion. We apply σ_i^z to the state with zero flux $|\psi\rangle_{GS}$, creating a Majorana fermion at site i and two fluxes at the plaquette sharing bond. By propagating the initial spin flip in time with time-evolution operator $e^{-iHt/\hbar}$ we get a linear combination of states with fixed Z_2 fluxes and dynamic Majorana fermions at any lattice site j [11].

Two states with different configurations of bond fermions (plaquette fluxes) are mutually orthogonal [11]. A state obtained by the action of a spin operator on the ground state is orthogonal to the ground state, hence all the expectation values $\langle \sigma_i^{\alpha} \rangle = 0$ are zero. Consequently, there is no magnetization $M_{\alpha} = \frac{1}{N}\sum_i \langle \sigma_i^{\alpha} \rangle$ in the spin-liquid ground state. The physics of the Kitaev model in the spin liquid ground state has some similarities with antiferromagnetic states and valence bond solids formed by spin singlets, however, is fundamentally different:

1. The antiferromagnetic state also exhibits zero magnetization $M_{\mathrm{AFM}} = 0$, however, the expectation value of the spin operator at any given site $\langle \sigma_i^{\alpha} \rangle$ is not zero as opposed to the Kitaev model.

2. In the valence bond solid all expectation values of spin operators are zero due to formation of spins in singlet pairs, however, the Kitaev spin liquid exhibits different two-spin correlations $S_{ij}^{\alpha} = \left\langle \sigma_i^{\alpha} \sigma_j^{\alpha} \right\rangle$. In the ground state of the Kitaev model only neighbouring spins are correlated,

since the pair of fluxes, created by the first spin σ_j^α, must be annihilated by the second spin σ_i^α to obtain a non-zero expectation value. In the valence bond solid only spins, belonging to the same singlet pair, are correlated, whereas any two spins in different singlets yield zero correlation [11].

5. Experimental realization of the Kitaev model

Quantum spin liquid states of matter are very difficult to detect experimentally, because they lack a local order parameter to which common experimental probes could couple directly. While long-range entanglement is not easily accessible by experiment, the fractionalization of the fundamental spin degrees of freedom could potentially be detected by means of thermodynamic and spin structure factor measurements [16]. Candidates for the experimental realizations of the Kitaev model were initially sought in honeycomb iridates Li_2IrO_3 and Na_2IrO_3, since they possess the characteristic bond-directional exchange interactions. However, due to strong structural distortions in iridates, other non-Kitaev interactions become significant, causing the magnetism to be dominated by antiferromagnetic ordering [2]. More promising candidate for the Kitaev spin liquid is a van der Waals material α-$RuCl_3$, consisting of weakly coupled honeycomb layers. These systems host predominantly bond-directional isotropic ($J_x = J_y = J_z$) Kitaev interactions. Significant advances in the synthesis of α-$RuCl_3$ crystals have enabled Sungdae Ji and collaborators [2] to experimentally observe signs of spin fractionalization. Their findings are based on specific heat measurements, which are supported from results of inelastic neutron scattering, used to determine the dynamic structure factor [2]. The measured temperature dependence of the magnetic specific heat C_M unveils a two-stage release of magnetic entropy S_M that suggests an existence of two types of excitations; localized Z_2 fluxes and itinerant Majorana fermions, which are thermally activated at different temperatures. Below $T_N = 6.5$ K, non-vanishing interlayer couplings in α-$RuCl_3$ cause the spins to order in an antiferromagnetic structure. Despite theoretical predictions, absence of magnetic order was not observed when approaching $T = 0$ K [16]. A suggested physical interpretation of the phase diagram for α-$RuCl_3$ is shown in Figure 9.

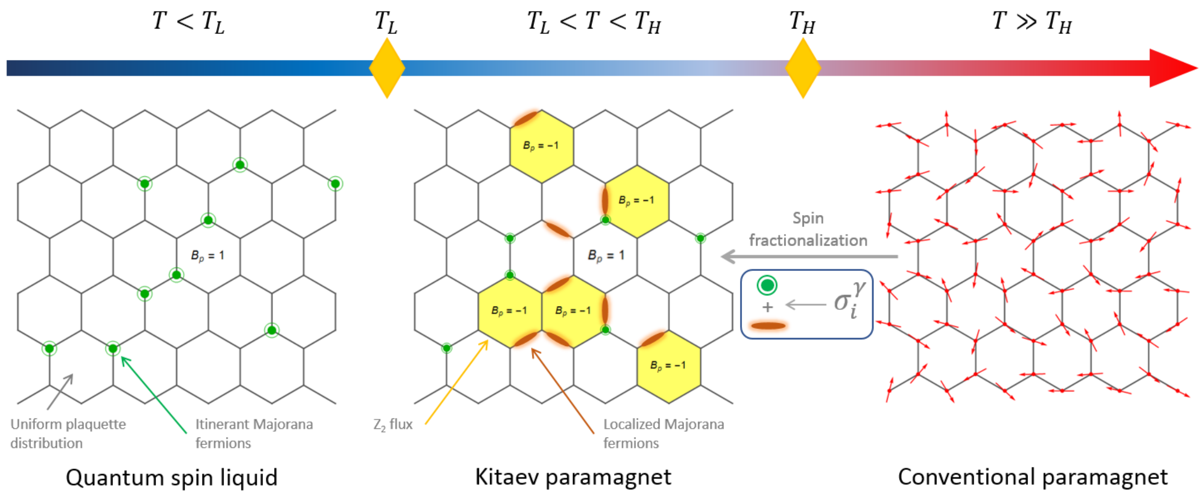

Figure 9. (Left) At very low temperatures $T < T_L$, but above the transition temperature T_N to the magnetically ordered state, only low-energy itinerant Majorana fermions (green circles) are thermally activated, whereas the static Z_2 fluxes remain frozen in uniform configuration ($B_p = 1$), forming a quantum spin liquid state. **(Middle)** Upon increasing the temperature across T_L, the Z_2 fluxes ($B_p = -1$) begin to form along with localized Majorana fermions (orange ovals) on the bonds, forming a Kitaev paramagnet. **(Right)** Finally, above the high temperature crossover T_H, the system becomes a conventional paramagnet [2].

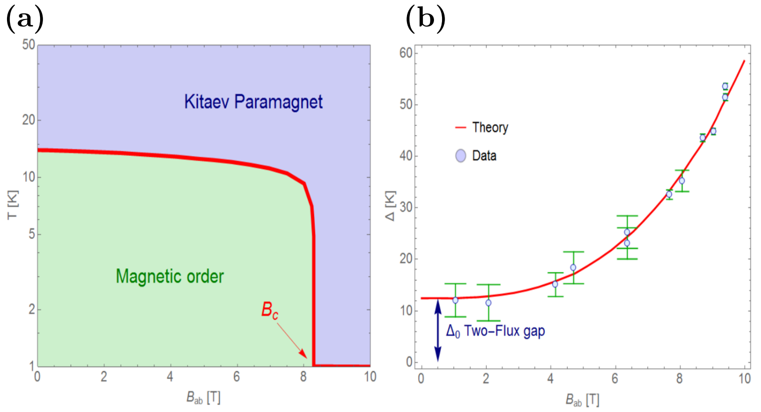

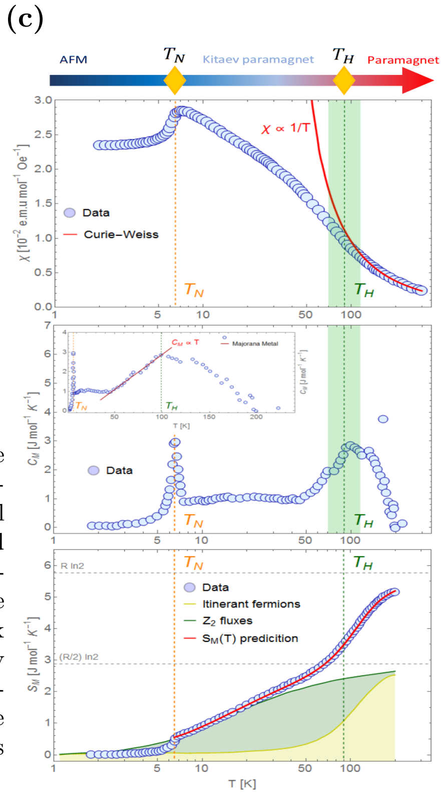

Figure 10. **(a)** Phase diagram of α-$RuCl_3$ showing the extent of the magnetically ordered antiferromagnetic phase as a function of temperature T and the effective magnetic field B_{ab}. The effect of any external field can be namely reduced to an action of the effective magnetic field within the plane of the sample. (Reproduced from [17].) **(b)** Spin excitation gap Δ as a function of the effective magnetic field B_{ab} follows the theoretically predicted cubic growth and reproduces the initial two-flux gap Δ_0 at zero field. (Reproduced from [17].) **(c)** Magnetic susceptibility $\chi(T)$, specific heat C_M and magnetic entropy S_M as a function of temperature T. Entropy release is decomposed into two components that are activated at different temperatures and correspond to itinerant fermions (T_H) and Z_2 fluxes (T_L). (Reproduced from [2].)

Signatures of spin fracitonalization were seen in measurements of the magnetic susceptibility $\chi(T)$, specific heat C_M and magnetic entropy $S_M = \int C_M/T \, \mathrm{d}T$ (Figure 10.c). Especially the two stage release of the magnetic entropy signifies two types of excitations in the system, however, the low-temperature spin liquid phase is obscured by formation of antiferromagnetic order. Some Z_2 flux excitations of the uniform configuration are already formed at temperatures slightly above T_N. Anomalies of the susceptibility and a sharp peak of C_M indicate a phase transition at T_N, where the system orders antiferromagnetically. In the intermediate region C_M has a linear T-dependence, reflecting the metallic behaviour of itinerant Majorana fermions. Another peak was detected at T_H, where conventional paramagnetic phase is formed [2]. Another indication of spin fracitonalization is an energy gap Δ_0 created by a spin flip, which is accompanied by creation of a pair of fluxes. In the external field B, the gapless phase also acquires a gap, which is predicted to grow with the third power of the field B (Figure 10.b). Field dependence of the spin excitation gap Δ is determined by the spin-lattice relaxation time measured using nuclear magnetic resonance [17]. The ordered antiferromagnetic phase in α-$RuCl_3$ disappears when we apply a significantly strong external magnetic field that overwhelms the additional anisotropic exchange couplings between spins, which give rise to the ordering at lower magnetic fields [17] (Figure 10.a).

6. Conclusion

Frustrated magnetic systems governed by strong fluctuations present an interesting playground, where new exotic quasiparticle excitations might be found. The Kitaev spin model is especially remarkable, since it can be theoretically solved and predicts a quantum spin liquid ground state as well as fractionalization of spin degrees of freedom into Majorana fermions and static Z_2 gauge fluxes. Furthermore, the flux excitations in the gapped phase and excitations in the presence of the external magnetic field even obey anyonic statistics. Experimentalists have been pursuing signs of fractionalization and exotic quasiparticle excitations in a variety of condensed-matter systems.

The main benefit of the discussed Kitaev material α-$RuCl_3$ is the fact that spin fractionalization is observed in a broad temperature range, whereas in fractional quantum Hall effect it was seen only at extremely low temperatures and for certain field values [17]. The discussed Majorana fermions were also observed as excitations in thermal quantum Hall effect [18]. Basic feature of anyons in 2D, which distinguishes them from more familiar quasiparticles, is their memory of knotted world lines in space-time. The knotted topology makes anyons very stable in a wide temperature range, since they are extremely resistant to distortions from the environment. Many-anyon systems could build up a stable collective memory, which can serve as a platform for topological quantum computing. Computing with anyons could exploit their ability to map their knotted histories into (observable) quantum-mechanical amplitudes [1]. In the external magnetic field, the Kitaev honeycomb model hosts non-Abelian anyonic excitations with potential applications in quantum computing. Moreover, experimental observations of fractionalized excitations in α-$RuCl_3$ suggest that a good solid-state realization of the Kitaev model, with little distortions from other non-Kitaev interactions, has been found.

Acknowledgements

I would like to thank my mentor doc. dr. Martin Klanjšek for introducing me to the physics of quantum spin liquids and his support, comments and constructive criticism while writing this article.

REFERENCES

[1] F. Wilczek, *Inside the Knotty World of 'Anyon' Particles*, Quanta Magazine, `https://www.quantamagazine.org/how-anyon-particles-emerge-from-quantum-knots-20170228/`, 2017, Accessed: 24-02-2022.

[2] S. Do, S. Ji et al., *Incarnation of Majorana Fermions in Kitaev Quantum Spin Lattice*, arXiv: 1703.01081.

[3] F. Schwabl, *Advanced Quantum Mechanics*, 4 ed., Springer, Berlin, Germany, 2008.

[4] P. Ball, *Making anyon soup*, Nature Materials **16** (2017), 706.

[5] N. Ashcroft and D. Mermin, *Solid State Physics*, Saunders College Publishing, 1976.

[6] R. de-Picciotto et al., *Direct observation of a fractional charge*, Nature **389** (1997), 162–164.

[7] *Quantum spin liquid*, Wikipedia, `https://en.wikipedia.org/wiki/Quantum_spin_liquid`, 2022, Accessed: 24-02-2022.

[8] S. Trebst and C. Hickey, *Kitaev Materials*, Physics Reports **950** (2022), 1-38.

[9] P. W. Anderson, *Resonating valence bonds: A new kind of insulator?*, Materials Research Bulletin **8** (1973), 153-160.

[10] L. Balents, *Spin liquids in frustrated magnets*, Nature **464** (2010), 199–208.

[11] A. Kitaev, *Anyons in an exactly solved model and beyond*, Annals of Physics **321** (2006), 2–111.

[12] *Mott insulator*, Wikipedia, `https://en.wikipedia.org/wiki/Mott_insulator`, 2022, Accessed: 24-02-2022.

[13] G. Khaluillin and G. Jackeli, *Mott Insulators in the Strong Spin-Orbit Coupling Limit: From Heisenberg to a Quantum Compass and Kitaev Models*, Physical Review Letters **102** (2009), 017205.

[14] G. Baskaran, S. Mandal, S. Shankar, *Exact Results for Spin Dynamics and Fractionalization in the Kitaev Model*, Physical Review Letters **98** (2007), 247201.

[15] A. Kitaev, *Fault-tolerant quantum computation by anyons*, Annals of Physics **303** (2003), 2-30.

[16] N. Perkins, *Kitaev physics crystalized*, Nature Physics **13** (2017), 1041–1042.

[17] N. Janša, M. Klanjšek et al., *Observation of two types of anyons in the Kitaev honeycomb magnet*, arXiv: 1706.08455v2.

[18] Y. Kasahara, T. Ohnisi et al., *Majorana quantization and half-integer thermal quantum Hall effect in a Kitaev spin liquid*, Nature **559** (2018), 227–231.